Chemical Science

RSC Publishing

EDGE ARTICLE

View Article Online
View Journal | View Issue

Cite this: *Chem. Sci.*, 2013, **4**, 3484

Probing chemistry and kinetics of reactions in heterogeneous catalysts

Tristan G. A. Youngs,*[a] Haresh Manyar,[b] Daniel T. Bowron,[a] Lynn F. Gladden[c] and Christopher Hardacre*[b]

Received 25th May 2013
Accepted 16th June 2013

DOI: 10.1039/c3sc51477c

www.rsc.org/chemicalscience

Using benzene hydrogenation over Pt/SiO_2 as an industrially-relevant example, we show that state-of-the-art neutron total scattering methods spanning a wide *Q*-range now permit relevant time-resolved catalytic chemistry to be probed directly *in situ* within the pore of the catalyst. The method gives access to the reaction rates on both nanometric and atomic length scales, whilst simultaneously providing an atomistic structural viewpoint on the reaction mechanism itself.

Introduction

Catalysis in general, and heterogeneous catalysis in particular, is critical to the production of chemicals worldwide. It has been estimated that ~80% of all man made materials at some point in their manufacture use a catalyst[1] and the majority of these are heterogeneously catalyzed reactions. As a consequence of their importance, it is thought that ~35% of the world's GDP is reliant on catalysis.[2] Many of these reactions are performed in the liquid phase; however, despite the importance of these materials and processes, the understanding of multi-phase interfaces and the impact of these on the overall rate process is poor. Liquid phase heterogeneously catalyzed reactions are commonly monitored using liquid sampling or gas uptake due to the difficulty of obtaining *in situ* spatially- and chemically-resolved information on the microscopic scale. Although nuclear magnetic resonance techniques can obtain spatially-resolved activity and diffusion information within packed-bed systems,[3,4] these methods are limited to micron resolution. Neutron scattering is an excellent atomic probe of condensed matter; however, until now, long data acquisition times have prevented total scattering techniques from being used to measure the kinetics of real systems. Small angle X-ray and neutron scattering has been applied to time-resolved studies of, for example, micelle aggregation[5] and evolution,[6] rheochaos and flow instability,[7] and polymerisation processes,[8] but the nature of these techniques necessarily means that information in the atomistic and chemical regime is lacking. Herein, we demonstrate that wide *Q*-range, total neutron scattering at state of the art pulsed neutron facilities is now able to obtain kinetic information of reaction processes over multiple length scales spanning the small angle and wide angle regimes simultaneously.

In this study, the platinum-catalysed hydrogenation of benzene to cyclohexane has been used as a proof of principle that neutron methods can probe the reaction within the pore of the catalyst. Benzene hydrogenation has been studied extensively in both the liquid phase and vapour using a range of catalysts including supported Ru,[9] Fe,[10] Pd,[11] Ni[12] and Pt[13] with a view to understand the mechanism of the reaction. This reaction is of particular commercial importance due to the widespread use of the product (cyclohexane) as a precursor in the production of adipic acid and caprolactam en-route to the eventual production of nylon as well as the drive for cleaner fuels and the removal of benzene from gasoline.

Experimental details

Neutron diffraction

The structural quantity measured in a total scattering experiment is the interference differential cross section, $F(Q)$, where Q is the magnitude of the momentum transfer vector in the scattering process for neutrons of incident wavelength (λ) and scattering angle (2θ), defined as:

$$Q = \frac{4\pi}{\lambda}\sin\theta \quad (1)$$

$F(Q)$ is formed from a weighted sum of the partial structure factors, $S_{ij}(Q)$ that reflect the pair correlations between atoms of type i and j:

$$F(Q) = \sum_{i,j}(2-\delta_{ij})c_i c_j b_i b_j (S_{ij}(Q)-1) \quad (2)$$

δ_{ij} is the Kronecker delta to avoid double counting the pair terms, and c_i, c_j and b_i, b_j are the atomic fractions and coherent scattering lengths of the atom types. The interference

[a]*ISIS Facility, STFC Rutherford Appleton Laboratory, Harwell Oxford, Didcot, Oxfordshire, OX11 0QX, UK. E-mail: tristan.youngs@stfc.ac.uk; Tel: +44 (0)1235 445050*

[b]*CenTACat, School of Chemistry and Chemical Engineering, Queen's University Belfast, Belfast, BT9 5AG, UK. E-mail: c.hardacre@qub.ac.uk; Tel: +44 (0)2890 974592*

[c]*Department of Chemical Engineering and Biotechnology, University of Cambridge, Cambridge, CB2 3RA, UK*

differential cross section is related by Fourier transform to the corresponding radial distribution function, $G(r)$, weighted by the atomic density of the system, ρ:

$$G(r) = \frac{1}{(2\pi)^3 \rho} \int_0^\infty 4\pi Q^2 F(Q) \frac{\sin Qr}{Qr} \mathrm{d}Q \quad (3)$$

$G(r)$ is formed from a weighted sum of the partial pair distribution functions, $g_{ij}(r)$, in similar fashion to $F(Q)$ (eqn (2)). When investigating nanostructured materials, as in the present case, it is often preferable to use the differential correlation function $D(r)$, derived from the radial distribution $G(r)$ as:[14]

$$D(r) = 4\pi\rho r G(r) \quad (4)$$

This alternate form emphasizes the structural features at longer distances.

All neutron diffraction measurements were made on the Near and InterMediate Range Order Diffractometer[15] (NIMROD) at the ISIS Second Target Station Facility of the Rutherford Appleton Laboratory, Oxford, UK. NIMROD provides high flux and a wide Q range accessing correlations between <0.1 nm and ~30 nm. Of critical importance is the instrument's high neutron count-rate at molecular and intermediate order length scales which allows short acquisition times to be employed, thus facilitating the extraction of kinetic information. Benzene hydrogenation was performed using Pt/SiO_2 within the instrument at 296 K and 0.25 bar D_2(g). Therefore, to be precise, the measurements probed the deuteriation of benzene-d_6, Scheme 1, as the heavier isotope exhibits more favorable neutron scattering characteristics. Before the neutron diffraction was undertaken, the catalyst was prereduced by exposing the catalyst to D_2 in benzene-d_6 at room temperature. This mixture was then pumped from the system until the diffraction pattern of the catalyst did not change and then the catalyst pore was refilled with benzene-d_6 vapour and then D_2.

Synthesis

All chemicals, unless otherwise stated, were purchased from Aldrich or Qmx and used without further purification. The mesoporous SiO_2 was synthesized by modification of a previously reported procedure by Grün *et al.*[16] 5 g of *n*-hexadecyltrimethylammonium bromide (C_{16}TMABr, 0.014 mol) was dissolved in 100 g of ultra-pure water (distilled, deionised >18 MΩ) by heating at 318 K, and 26.4 g of aqueous ammonia (32 wt%, 0.5 mol) and 120.0 g of absolute ethanol (EtOH, 2.6 mol) were added to the surfactant solution. The solution was stirred for 15 min and 9.4 g of triethyl orthosilicate (TEOS) (0.044 mol) was then added resulting in a gel with the molar composition $(TEOS)(C_{16}TMABr)_{0.3}(NH_3)_{11}(H_2O)_{144}(EtOH)_{58}$. After stirring for 2 h, the gel was transferred to a Teflon-lined autoclave and aged for 48 h at 378 K. The white precipitate obtained was filtered, washed with 200 cm^3 of ultra-pure water and 200 cm^3 of methanol and dried overnight at 363 K. The white powder was calcined in air at 823 K for 5 h (heating rate 2 K min^{-1}). 5 wt% Pt/SiO_2 was prepared by incipient wetness impregnation using platinum nitrate (Johnson-Matthey) as the platinum precursor. After impregnation, the material was dried at 393 K for 12 h followed by calcination at 773 K for 4 h.

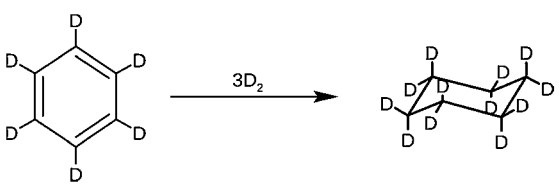

Scheme 1 Deuteriation of benzene-d_6 to cyclohexane-d_{12}.

Batch liquid phase hydrogenation of benzene

Benzene hydrogenation experiments were carried out in a 100 cm^3 Autoclave Engineers' high pressure reactor. In a typical experiment, the reactor was charged with 20 cm^3 of benzene and 0.25 g of 5 wt% Pt/MCM-41 catalyst. The reactor was purged three times with N_2, the mixture was agitated at 1500 rpm and heated to 323 K. After purging with H_2 three times, the reactor was pressurised to 5 bar, which corresponded to $t = 0$. The reaction was monitored by sampling at regular time intervals,

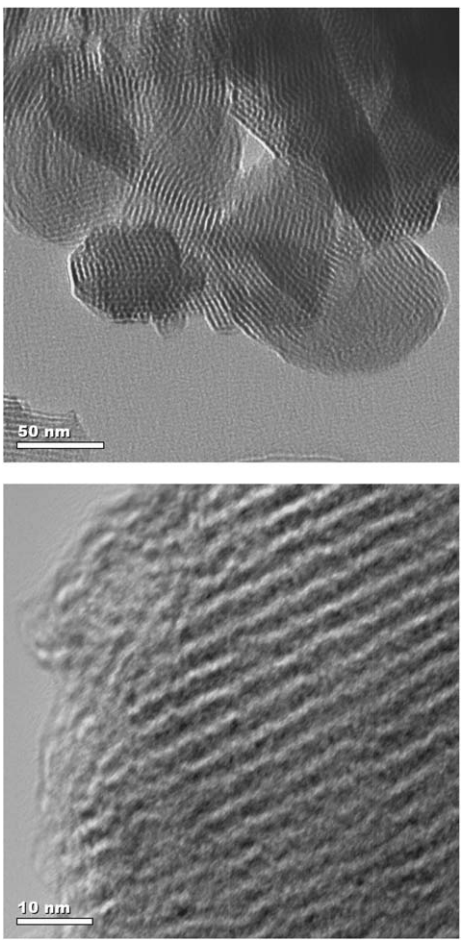

Fig. 1 HR-TEM images of the prepared catalyst, acquired in bright field using a Tecnai 200 kV F20 Transmission Electron Microscope with a Field Emission Gun.

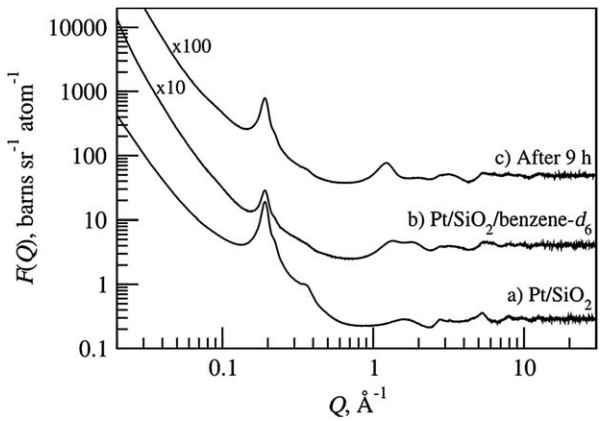

Fig. 2 Total differential cross scattering data ($F(Q)$) of dry Pt/SiO_2, the system after exposure to benzene-d_6 vapour, and the final system after 9 h reaction time. Error bars not shown since symbol height is comparable to line thickness.

with analysis of the samples by a Perkin Elmer GC equipped with a DB-1 capillary column and a FID detector. Under these conditions, 98% conversion of benzene was obtained after 24 h.

Catalyst characterisation

High resolution TEM images of the prepared catalyst, Fig. 1, show the expected regular hexagonal array of uniform parallel channels, while Pt nanoparticles (<1 nm in size) can be seen as dark spots dispersed within the channels.

In order to interpret the data of the complete system, careful textural characterization of the catalyst is critical. Traditionally, adsorption isotherms, *e.g.* BET, are employed to measure the porosity of these materials; however, these methods provide only a rough characterization.[17] Neutron methods are advantageous as they provide more comprehensive characterization with a single probe.[18]

Fig. 2 shows the $F(Q)$ obtained from evacuated Pt/SiO_2 from which a direct characterization of the porous framework can be obtained. Fitting a Lorentzian profile to the first diffraction peak gives a centre of 0.190 $Å^{-1}$ with FWHM of 0.022 $Å^{-1}$, corresponding to a pore spacing of 33.1 Å (s.d. 1.48 Å). Direct Fourier transform of the measured empty Pt/SiO_2 sample is given in Fig. 3, which show the differential correlation functions, $D(r)$. The spacing of the pores in the material ($d = 33$ Å) is clearly visible in the Pt/SiO_2 data, with oscillations of this period extending to beyond 100 Å. X-ray diffraction measurements on the same material suggest a d spacing of 34.6 Å, in good agreement with the neutron value.[19]

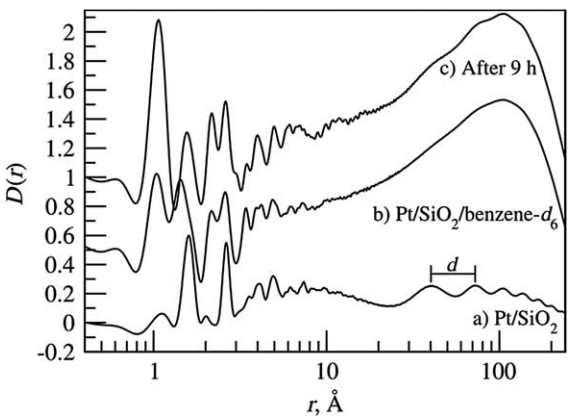

Fig. 3 Direct Fourier transforms of the data shown in Fig. 2. d corresponds to the pore spacing in the material. The underlying feature at large r apparent in the pore-filled systems is an artefact of the discrete Fourier transform process, arising from the unavoidable step function at the first data point ($Q = 0.01$ $Å^{-1}$).

Results and discussion

Reactant/product characterisation

Following measurement of the evacuated catalyst, benzene-d_6 was absorbed *via* capillary condensation of the vapour into the pores. After five minutes, saturation of the pores was achieved and no further changes in the structure factor observed (Fig. 2). This data shows a decrease in the intensity of the first diffraction peak together with an increase in complexity of the signal beyond 1 $Å^{-1}$. The former is consistent with the pores becoming filled with a material possessing a scattering length density (SLD), *i.e.* benzene-d_6, which offers less contrast to the silica than the evacuated pore. For deuteriated benzene, $\Delta SLD = 1.93 \times 10^{-6}$ $Å^{-2}$ compared with $\Delta SLD = 3.47 \times 10^{-6}$ $Å^{-2}$ for the empty pore thus reducing the contribution of pore–pore features in the $F(Q)$. The increased signal complexity above 1 $Å^{-1}$ is consistent with additional atomic-scale correlations corresponding to the absorbed benzene-d_6. In real space, the decrease in intensity of the first diffraction peak is matched by a 'washing out' of the periodic pore correlation (Fig. 3) – the oscillations at long r are almost completely damped because of contrast matching.

After exposure to D_2(g) for 9 h, the $F(Q)$ data (Fig. 2) show an increase in the first diffraction peak which is consistent with the

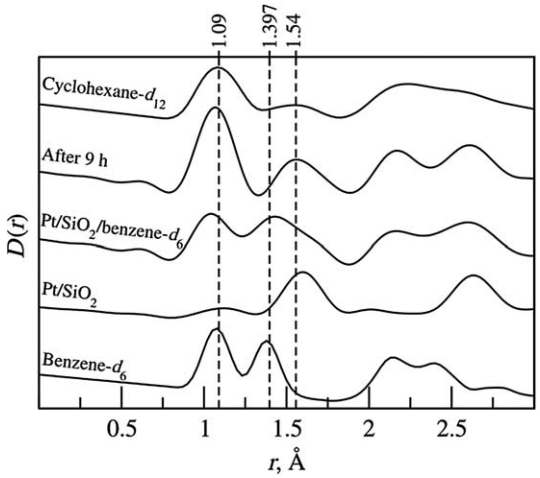

Fig. 4 Direct Fourier transforms of diffraction data in Fig. 2 along with those from measurements of neat benzene-d_6 and cyclohexane-d_{12}, focusing on the atomic pair correlations in the short r (chemical structure) region. Curves have been offset vertically for clarity. Positions of typical C–D (1.09 Å), aromatic C–C (1.397 Å), and aliphatic C–C (1.54 Å) are shown to aid interpretation. Note the decreased intensity at 1.397 Å and increased intensity at 1.09 and 1.54 Å in the system after 9 h reaction, indicating the hydrogenation of benzene.

formation of cyclohexane-d_{12} from the hydrogenation of benzene. Cyclohexane-d_{12} has a SLD which gives comparable contrast with the bulk SiO_2 to that of the empty pore, $\Delta SLD = 3.24 \times 10^{-6}$ *cf.* 3.47×10^{-6} Å^{-2}, thus promoting reappearance of the first diffraction peak. Consequently, the long *r* oscillations in the $D(r)$ are somewhat restored, Fig. 3. In addition, the presence of a strong feature at $Q = 1.2$ Å^{-1} suggests the presence of a species which is different from benzene and not found at $t = 0$. Fig. 4 shows the direct Fourier transform of the initial benzene-loaded system, the average of the last six datasets collected[20] corresponding to the final 0.5 h of the study where little further reaction occurs and those from the pure liquids. Both the benzene-loaded and pure benzene systems show C–C correlations at 1.397 Å but these are absent after reaction. Similarly, the new feature at ~1.55 Å is consistent with the cyclohexane C–C distance which overlaps with the Si–O peak at 1.59 Å associated with the porous catalyst. The data also display a marked increase in the intensity of the C–D peak after reaction indicating complete conversion of benzene. This was confirmed by extracting the discharged catalyst with *n*-hexane and analysis by GC-MS which showed only the presence of cyclohexane-d_{12}. This is consistent with the batch liquid phase reactions undertaken using this catalyst as well as literature data[21] which showed little formation of the intermediates cyclohexadiene or cyclohexene, and is in agreement with theoretical studies which suggest that these molecules are not part of the major reaction pathway.[22]

Time resolved data

The evolution of $F(Q)$ as a function of time, Fig. 5a, illustrates the changes within structural features across atomic, molecular, and mesoscopic length scales simultaneously. By taking

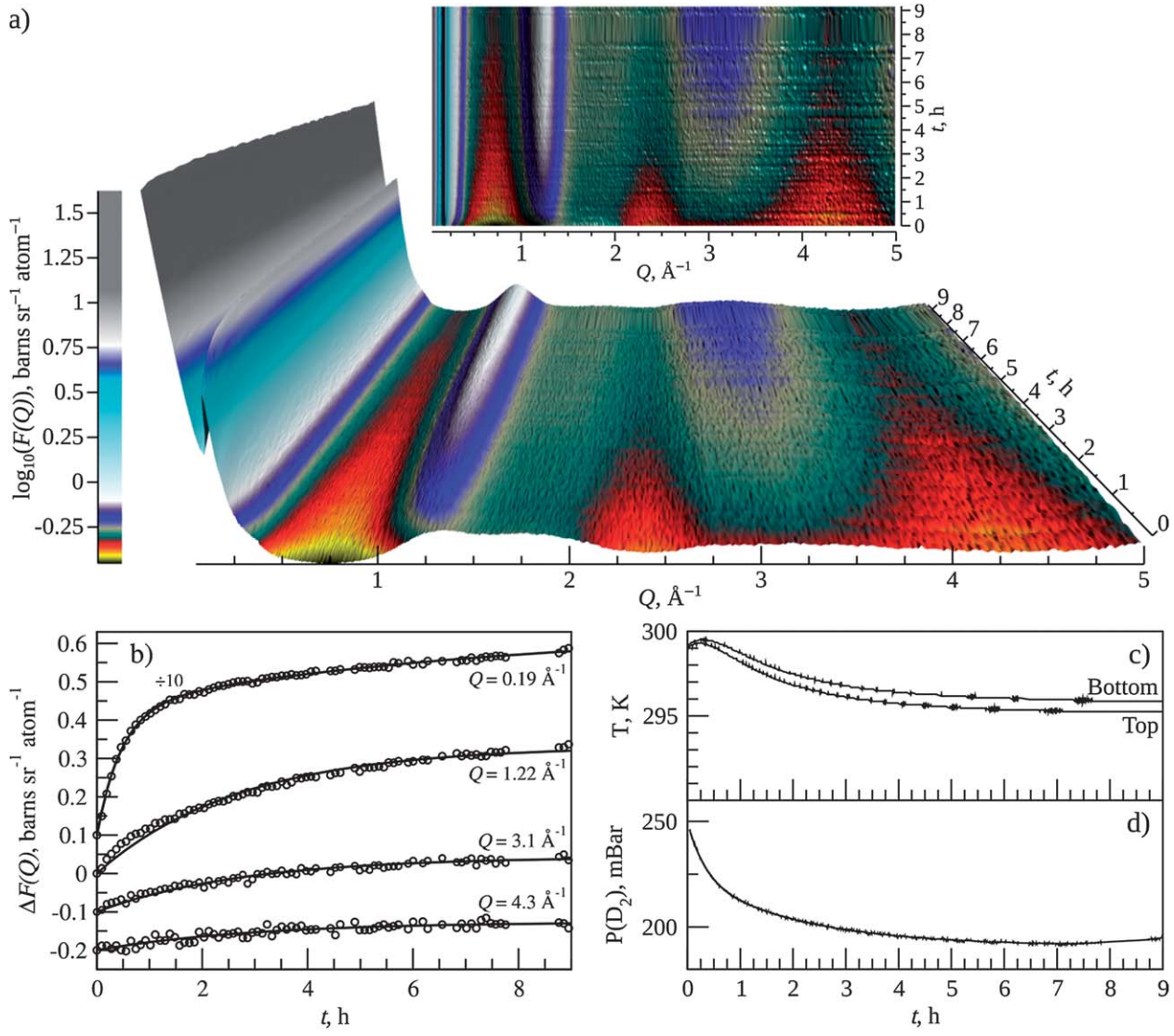

Fig. 5 (a) $F(Q)$/time domain data over the course of the reaction. (b) Slices taken through (a) at specific Q values, and corresponding exponential fits to the data. Curves are offset vertically for clarity. Fit equations are: $F(Q = 0.19) = (a_0 + a_1) - a_0\exp(-k_0t) - a_1\exp(-k_1t)$, where $a_0 = 3.584$, $a_1 = 2.234$, $k_0 = 2.146$ h^{-1}, and $k_1 = 0.136$ h^{-1}; $F(Q \neq 0.19) = a_n - a_n\exp(-k_nt)$, where $a_2 = 0.332$ and $k_2 = 0.368$ h^{-1} ($Q = 1.22$ Å^{-1}), $a_3 = 0.143$ and $k_3 = 0.361$ h^{-1} ($Q = 3.1$ Å^{-1}), and $a_4 = 0.074$ and $k_4 = 0.333$ h^{-1} ($Q = 4.3$ Å^{-1}). (c) Sample temperature as measured at the top and bottom extremes of the TiZr cell. (d) Pressure of D_2 gas present in 4 L supply reservoir.

slices at specific Q values with respect to time, the kinetics corresponding to different length scales in the system can be obtained, as shown in Fig. 5b (together with corresponding exponential fits). The first diffraction peak ($Q = 0.19$ Å^{-1}) exhibits both a fast (rate constant $k_0 = 2.146$ h^{-1}) and a slow ($k_1 = 0.138$ h^{-1}) component, while at $Q = 1.2$, 3.1, and 4.3 Å^{-1} the fits reveal an intermediate third rate ($k_{2,3,4} \approx 0.35$ h^{-1}). We have already established that the increase in intensity of the first diffraction peak is related to the change in contrast between the mesoporous substrate and absorbed material; however, a second process also contributes to this change on a different timescale. Inspection of the data ($1 < Q < 2\pi$ Å^{-1}) reveals no other changes which occur at a rate similar to the fast component (k_0). This first process is, therefore, unlikely to be related to benzene and is attributed to the dissociative adsorption of D_2. This is consistent with the rapid and relatively large increase in temperature over the first 30 minutes following introduction of the D_2, Fig. 5c. Similarly, the slow component (k_1) does not reflect a chemical change and is likely to be related to the mass transport of the products within the pore, *i.e.* pore diffusion. The change at $Q = 1.22$ Å^{-1} reflects nearest-neighbour molecular interactions, while those at $Q = 3.1$ and 4.3 Å^{-1} are associated with atomistic chemical changes within the system. These three features evolve with similar time constants and are correlated with the reduction process and the formation of the cyclohexane product. Moreover, these time constants suggest that the overall process is likely to be limited by liquid diffusion (k_1), as this is the slowest rate observed, whilst the reaction itself is governed by the hydrogenation process ($k_{2,3,4}$) rather than the dissociation of D_2 (k_0). From these results we are able to elucidate the following process scheme for the reaction, at conditions of room temperature and 250 mBar D_2:

$$D_{2(g)} \rightarrow 2D_{(ads)},\ k_0 = 2.146\ h^{-1}$$

$$C_6D_{6(l)} + 6D_{(ads)} \rightleftharpoons C_6D_{12(l)},\ k_{2,3,4} \approx 0.35\ h^{-1}$$

$$C_6D_{12(l)}\ \text{pore diffusion},\ k_1 = 0.136\ h^{-1}$$

Discussion

The necessity for more detailed information with respect to the kinetic evaluation of catalysts has been known for many years.[23] For example, there is a need to replace the ubiquitous concept of 'turnover frequency' (TOF) with a more quantitative measure[24] preferably with one whereby the rate equation for the system is known.[25] Such characterization has, in the past, been difficult, especially for liquid phase heterogeneously catalyzed processes since the rate law commonly contains several processes including both surface reaction and mass transport. Each has distinct rate constants, and no single technique has been able to comprehensively provide the necessary information. With this study total neutron scattering has been shown to be able to provide simultaneously the kinetic information associated with chemical reaction and mass transport within the pore of a catalyst. In the present case, the fact that pore liquid diffusion is critical in determining the rate of reaction is important in understanding how the catalyst design may be developed. Improvements in the surface reaction process, *i.e.* increasing the number or reactivity of the active sites, will have little influence on the catalyst performance whereas addition of a solvent, to increase the rate of diffusion, is likely to have a significant promoting effect. This proof of concept study has the potential to enable the temporal structure/spatial changes and the reaction kinetics to be correlated in the future, and therefore, obtain critical information pertaining to the catalytic process itself.

Conclusions

The kinetics within the pores of a heterogeneous catalyst during the liquid phase reduction of benzene have been probed directly using neutron diffraction, potentially providing a method of examining structure-reactivity correlations for these complex systems in detail, and thus allowing the effects of mass transport within the catalyst and surface reaction to be decoupled. Moreover, the technique takes a step to allow both structural and spatial data to be tied effectively with the kinetics of the underlying processes.

Acknowledgements

We thank the EPSRC and Johnson Matthey for funding under the CasTech project; M. Kibble and P. Hawkins for support during neutron diffraction experiments. Experiments at the ISIS Pulsed Neutron and Muon Source were supported by a beamtime allocation from the Science and Technology Facilities Council (experiment RB1220486, DOI: 10.5286/ISIS.E.24089729).

Notes and references

1 Z. Ma and F. Zaera, *Heterogeneous Catalysis by Metals in Encyclopedia of Inorganic Chemistry*, John Wiley, 2006.
2 F. Zaera, *Catal. Lett.*, 2012, **142**, 501.
3 E. H. L. Yuen, A. J. Sederman and L. F. Gladden, *Appl. Catal., A*, 2002, **232**, 29.
4 D. Weber, D. J. Holland and L. F. Gladden, *Appl. Catal., A*, 2011, **392**, 192.
5 J. Adelsberger, *Soft Matter*, 2013, **9**, 1685.
6 F. Michaux, N. Baccile, M. Impéror-Clerc, L. Malfatti, N. Folliet, C. Gervais, S. Manet, F. Meneau, J. S. Pedersen and F. Babonneau, *Langmuir*, 2012, **28**, 17477.
7 L. Gentile, B. F. B. Silva, S. Lages, K. Mortensen, J. Kohlbrecher and U. Olsson, *Soft Matter*, 2013, **9**, 1133.
8 R. Motokawa, T. Taniguchi, Y. Sasaki, Y. Enomoto, F. Murakami, M. Kasuya, M. Kohri and T. Nakahira, *Macromolecules*, 2012, **45**, 9435.
9 J. Bu, J. L. Liu, X. Y. Chen, J. H. Zhuang, S. R. Yan, M. H. Qiao, H. Y. He and K. N. Fan, *Catal. Commun.*, 2008, **9**, 2612; J. L. Liu, L. J. Zhu, Y. Pei, J. H. Zhuang, H. Li, H. X. Li, M. H. Qiao and K. N. Fan, *Appl. Catal., A*, 2009, **353**, 282.

10 K. J. Yoon, P. L. Walker, L. N. Mulay and M. A. Vannice, *Ind. Eng. Chem. Prod. Res. Dev.*, 1983, **22**, 519; K. J. Yoon and M. A. Vannice, *J. Catal.*, 1983, **82**, 457.
11 U. K. Singh and M. A. Vannice, *AIChE J.*, 1999, **45**, 1059; P. Chou and M. A. Vannice, *J. Catal.*, 1987, **107**, 140; P. Chou and M. A. Vannice, *J. Catal.*, 1987, **107**, 119; M. A. Vannice and W. C. Neikam, *J. Catal.*, 1971, **23**, 401; P.-H. Jen, Y.-H. Hsu and S. D. Lin, *Catal. Today*, 2007, **123**, 133.
12 K. C. Metaxas and N. G. Papayannakos, *Chem.–Eur. J.*, 2008, **140**, 352; M. Peyrovi and M. Toosi, *React. Kinet. Catal. Lett.*, 2008, **94**, 115; P. G. Savva, K. Goundani, J. Vakros, K. Bourikas, C. Fountzoula, D. Vattis, A. Lycourghiotis and C. Kordulis, *Appl. Catal., B*, 2008, **79**, 199.
13 D. Poondi and M. A. Vannice, *J. Catal.*, 1996, **161**, 742; S. D. Lin and M. A. Vannice, *J. Catal.*, 1993, **143**, 539; V. V. Pushkarev, K. An, S. Alayoglu, S. K. Beaumont and G. A. Somorjai, *J. Catal.*, 2012, **292**, 64.
14 D. A. Keen, *J. Appl. Crystallogr.*, 2000, **34**, 172.
15 D. T. Bowron, A. K. Soper, K. Jones, S. Ansell, S. Birch, J. Norris, L. Perrott, D. Riedel, N. J. Rhodes, S. R. Wakefield, A. Botti, M.-A. Ricci, F. Grazzi and M. Zoppi, *Rev. Sci. Instrum.*, 2010, **81**, 033905.
16 M. Grün, I. Lauer and K. K. Unger, *Adv. Mater.*, 1997, **9**, 254.
17 D. T. Bowron and A. K. Soper, *Neutron News*, 2011, **22**, 12.
18 A. K. Soper, *J. Phys.: Condens. Matter*, 2012, **24**, 064107.
19 X-ray diffraction measurements were made with Cu Kα radiation (1.5405 Å) on a PANalytical X'PERT PRO MPD diffractometer equipped with reflection geometry, a NaI scintillation counter, a curved graphite crystal monochromator and a nickel filter. The scattered intensities were collected from 1.5° to 6° (2θ) by scanning at 0.017° (2θ) steps with a counting time of 0.5 s at each step. No peaks due to Pt were observed due to the small Pt crystallite size.
20 Direct Fourier transform of the individual five minute datasets is challenging, owing to the reduced statistics in the high Q regime, therefore, several datasets have been summed to increase the signal to noise ratio.
21 For example, T. Bera, J. W. Thybaut and G. B. Marin, *Ind. Eng. Chem. Res.*, 2012, **50**, 12933.
22 M. Saeys, M.-F. Reyniers, M. Neurock and G. B. Marin, *J. Phys. Chem. B*, 2005, **109**, 2064.
23 B. W. Wojciechowski, *Chem. Innovation*, 2000, **30**, 47.
24 S. Kozuch and J. M. L. Martin, *ACS Catal.*, 2012, **2**, 2787.
25 G. Lente, *ACS Catal.*, 2013, **3**, 381.